Some Effects of Applied Stress on Early Stages of Cavitation Damage[1]

DALE J. KEMPPAINEN

General Electric Company

FREDERICK G. HAMMITT

University of Michigan

The problem of material attrition due to the phenomenon of cavitation has become increasingly important in recent years. Methods of alleviating cavitation damage have been suggested, including the use of externally applied stresses. The possible presence of inherent tensile or compressive stresses in fluid system components causes concern regarding their effect on the longevity of the components of the system as a whole when exposed to cavitation. Previous work from this laboratory (ref. 1) indicated that the effect of stress upon cavitation damage rates depended strongly upon the material. In general, compression, if applied parallel to the surface, tended to reduce the damage, while tension tended to increase it. The present paper considers particularly the initial phases of damage and the effect of these external stresses on the extent to which damage is incurred.

EXPERIMENTAL FACILITIES

General

Three experimental facilities were used to procure the data required for this study. These were (1) water loop with venturi, (2) mercury loop with venturi, and (3) vibratory facility (stationary specimen, nonflow system). Each of these facilities has been extensively discussed elsewhere (refs. 2–5). A short description of each system is given here only for clarification of test conditions. Reference 2 presents full details.

[1] Financial support provided by National Science Foundation Grant GK-1889.

Water Loop

The water loop, a multiple, closed-loop system, is shown in figure 1. One of the available loops was operated at a venturi throat velocity of 50 ft/sec at 75° F in the $\frac{1}{2}$-in.-diameter throat.

Mercury Loop

The mercury loop (fig. 2) is a single-loop venturi system. A throat velocity of 30 ft/sec at 75° F in the $\frac{1}{2}$-in.-diameter throat was used.

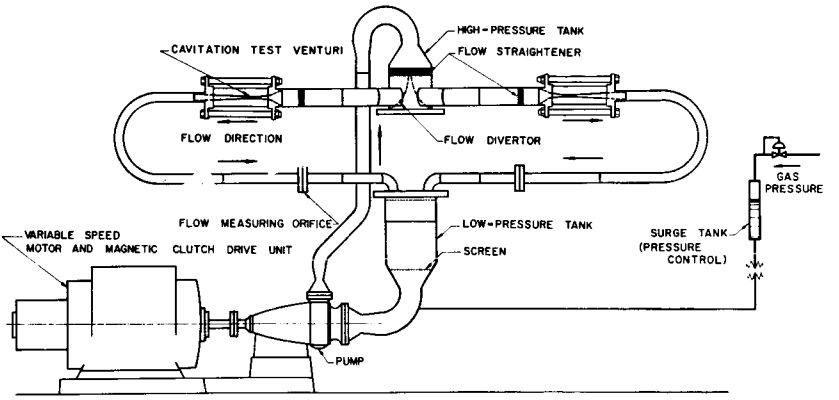

FIGURE 1.—*Schematic of water cavitation damage facility (only two of the four loops shown).*

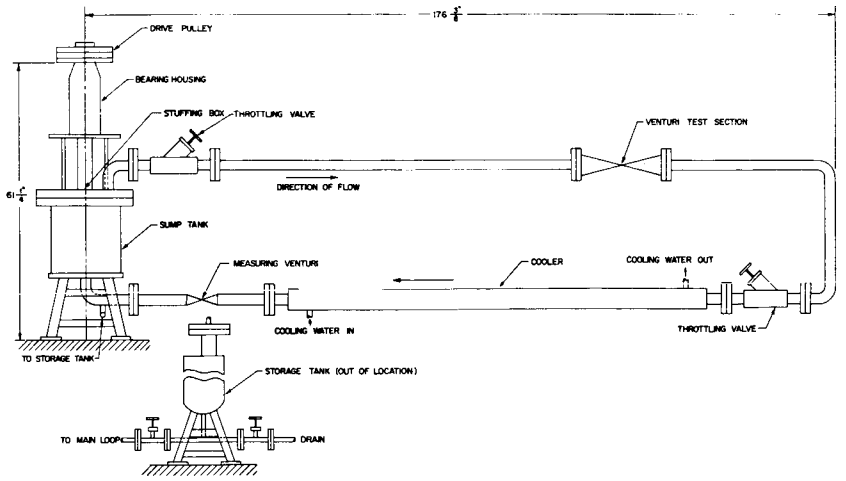

FIGURE 2.—*Schematic drawing of overall mercury facility layout.*

Vibratory Facility

A standard exponential horn (20 kHz, 2 mil) was used. The test specimens were held stationary in the cavitation field about 18 mils from the oscillating horn tip. Figure 3 is a schematic diagram of one of the arrangements used, and figure 4 illustrates the other.

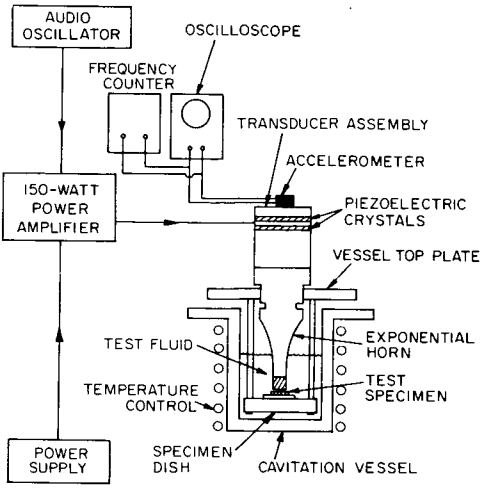

FIGURE 3.—*Schematic representation of the stationary-specimen vibratory cavitation test facility.*

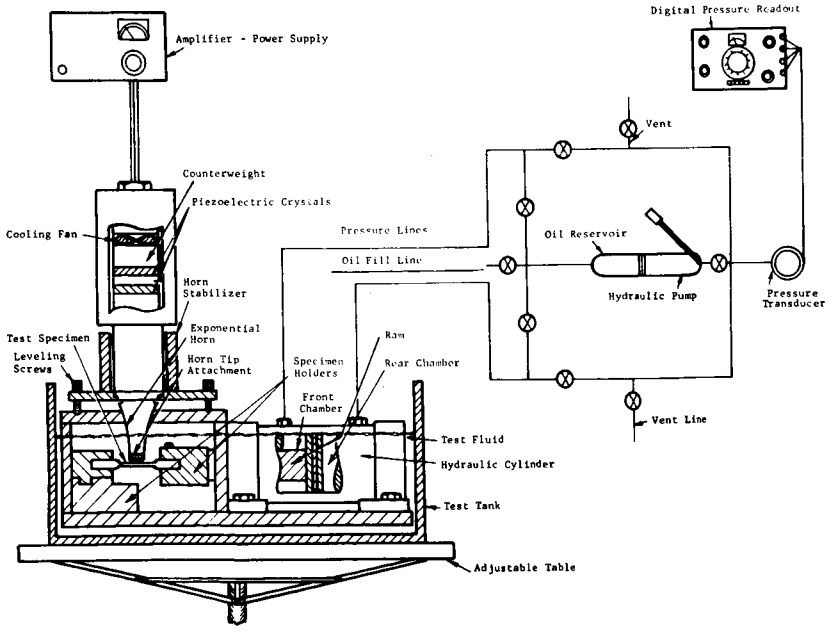

FIGURE 4.—*Schematic diagram of test facility.*

Specimen Placement

In both flowing systems a cylindrical specimen (fig. 5) was used. The specimen was placed across the fluid stream in the venturi diffuser (fig. 6), slightly downstream from the venturi throat exit.

Two types of specimens were used in the vibratory facility, depending on the method used to provide the applied stress: (1) 1.25-in.-diameter slugs placed parallel to the face of the vibratory horn or (2) a specimen of dumbbell shape closely resembling a tensile test specimen (fig. 7). Figure 4 shows the specimen arrangement. These tests were run in distilled water at 73° F.

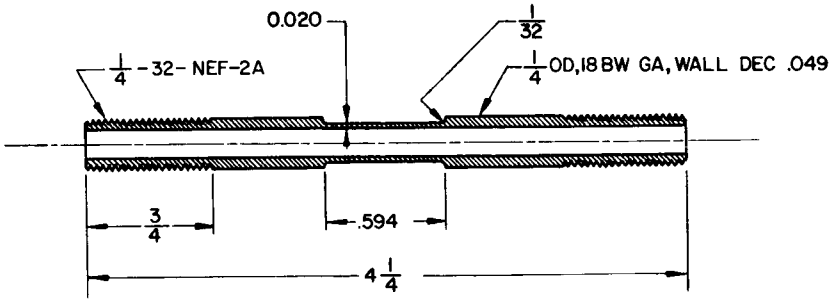

FIGURE 5.—*Drawing of tubular test specimen (pin).*

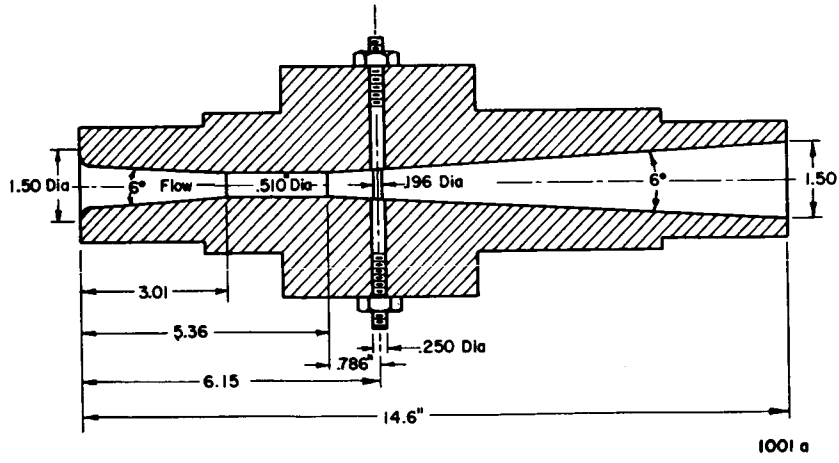

FIGURE 6.—*Assembly drawing of tension-test venturi.*

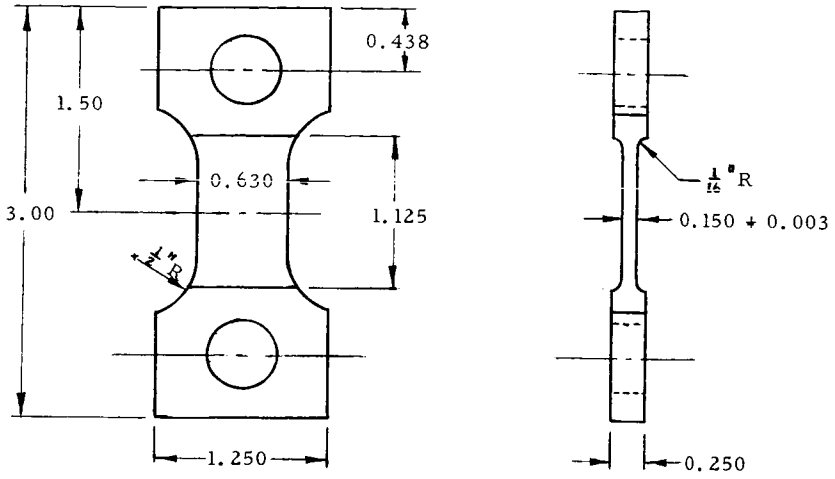

FIGURE 7.—*Dimensional drawing of tension/compression specimen.*

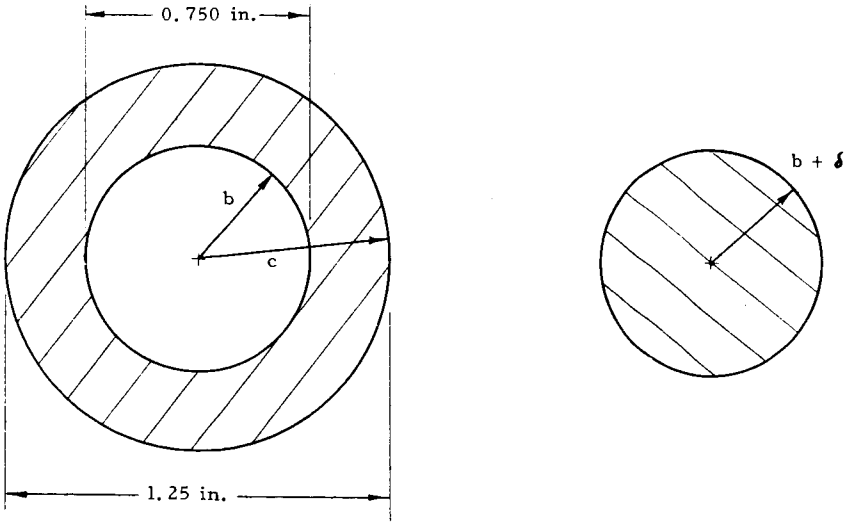

FIGURE 8.—*Test specimen and ring.*

Effect of Radially Symmetric Compressive Stress (Arrangement No. 1)

The first arrangement provides a radially symmetric compressive surface stress which corresponds to the radially symmetric flow of the fluid imposed by the oscillating horn tip (ref. 2). This stress field was provided by shrink-fitting an outer ring around the metal center (fig. 8).

The test specimen consisted of a solid cylindrical center section nominally 0.25 in. thick and 0.7500±0.0005 in. in diameter of the material to be tested. The outer ring was of type 304 stainless steel. By adjusting the radial interference, δ, the calculated specimen stress is varied according to the relationship:

$$P_{sf}=\frac{\delta/b}{1/E_0\{[1+(b/c)^2]/[1-(b/c)^2]+\nu_0\}+[(1-\nu_I)/E_I]}$$

where P_{sf} = compressive stress on the specimen material
E_0 = elastic modulus of the ring material
E_I = elastic modulus of the test material
ν_0 = Poisson's ratio for the outer material
ν_I = Poisson's ratio for the test material
$b+\delta$ = test specimen radius
δ = radial interference
c = outside radius of the outer ring
b = inside radius of the ring

The specimen and ring combinations were selectively paired according to the difference of fit, δ, after accurate measurement of the diameters, thus providing the desired surface compressive stress to the inner slugs.

Materials

Test materials were chosen which exhibited good reproducibility and availability, ease of fabrication, and relatively low damage resistance. Two materials, chosen to obtain rapid damage to investigate the feasibility of the test, were O.F.H.C. (oxygen-free high-conductivity) copper and 2024 aluminum. Control specimens of these materials were also made to the same diameter as the total test/slug/ring combination. Thus the same flow conditions were maintained for both the controls and the compressively loaded specimens.

TEST RESULTS

Damage Rates

Figure 9, which shows test data obtained for the shrink-fit specimens, indicates that the cavitation damage resistance of both the O.F.H.C. copper and the 2024 aluminum are decreased by the impressed radially symmetric compressive stress. This comparison, made on the basis of maximum volumetric loss rates, shows a 19.3-percent increase in damage over the nonstressed control for the copper and a 7.1-percent increase for the aluminum. However, the initial damage rate (i.e., that between time zero and 15 minutes) for the aluminum of the compressed specimen was

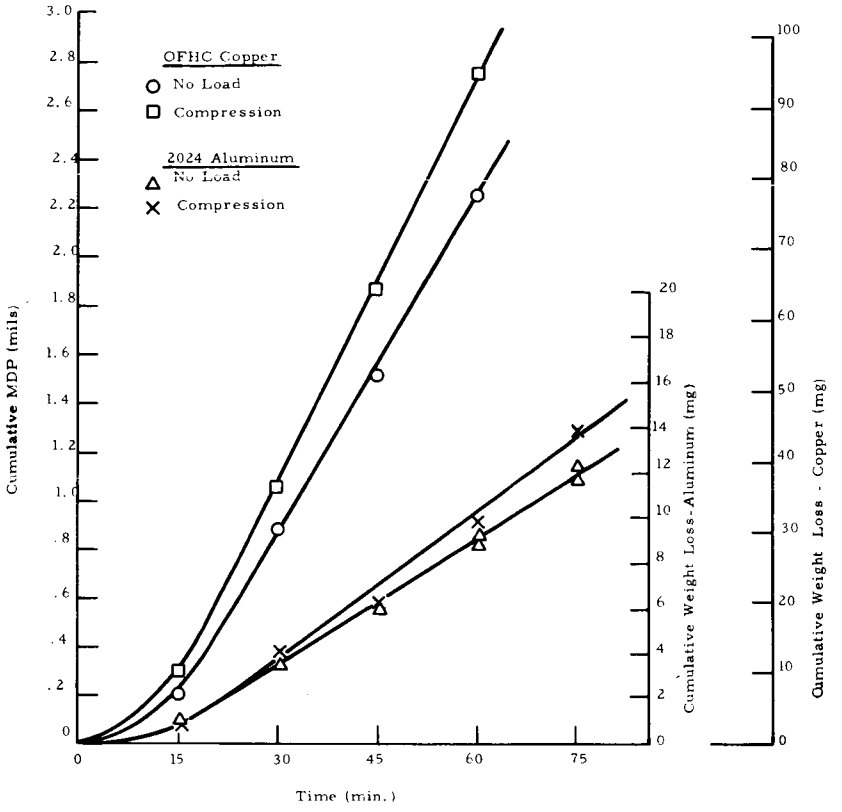

FIGURE 9.—*Effect of compressive stress on cumulative damage of O.F.H.C. copper and 2024 aluminum shrink-fit specimens.*

less than that for the nonstressed specimen. This same effect was reported earlier (refs. 1 and 2) for a number of other materials stressed only in the axial direction. For this particular material, in this test, for a mean depth of penetration (MDP[1]) less than 1 mil, the effect of the radially symmetric compressive stress was thus to inhibit the amount of cavitation damage. For greater MDP the damage rate increases, indicating that after

[1] MDP = mean depth of penetration (i.e., the volume loss per unit area, or an equivalent damage depth if volume loss were uniform across the entire area).

$$\text{MDP} = \frac{W}{\rho A}$$

where W = weight loss
ρ = density
A = damage area over which weight loss occurs

the initial damage period the inhibiting effect of the compressive stress decreases and then becomes negative. Thus the compressive stress appears to be detrimental once the surface of the material has been broken.

These same trends were not seen in the copper. However, no measurements for less than 0.1 mil MDP were made.

Photographic Investigation of Short-Duration Damage Tests

The results of a photographic investigation of specimens under the three load conditions of tension, compression, and zero applied load are shown in figure 10. These three series of photographs are a composite of 10-degree segments of a cylindrical specimen of type 304 stainless steel (fig. 5) run in the mercury loop (fig. 2). The test duration was 1.5 minutes with a throat velocity of 30 ft/sec and a pressure drop across the venturi of 71 psi. The pitting density changes which are evident from sector to sector are due to the distribution of the cavitation field which surrounds the specimen in this configuration (ref. 6). Figure 10*a* shows a polished 304 stainless-steel specimen tested with zero applied stress. Figure 10*b* shows the same material tested under a compressive load parallel to its

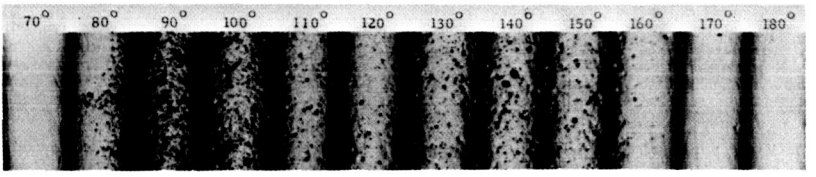

a.—*No applied force.*

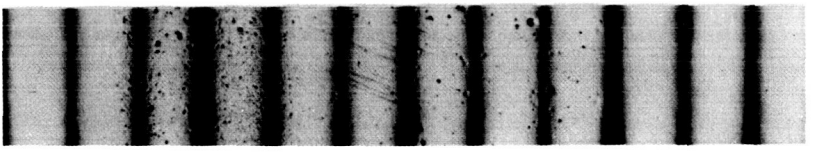

b.—*Compressive force.*

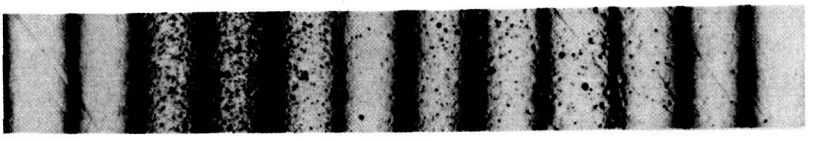

c.—*Tensile force.*

FIGURE 10.—*Effect of surface stress on damage for short-duration tests.*

axis of 88 percent of its yield strength, while figure 10*c* is for an impressed tensile load of 88 percent of the yield strength.

Comparing the photo for the imposed compressive force (fig. 10*b*) to that for zero force (fig. 10*a*) shows a very significant reduction in the number of smaller size pits and some reduction for all pits for compressive load. There are, however, still some very large pits visible in the compressive specimen. The tensile specimen (fig. 10*c*) and the zero-force specimen (fig. 10*a*) appear to be quite similar in pit-number densities of all sizes.

Three highly polished brass (65/35) specimens were run in the vibratory rig under conditions of tensile, zero, and compressive external applied load. The test duration in each stress mode was 10 seconds. The results are shown in figure 11. As in figure 10, there is markedly less pitting for compressive applied load than for other conditions. Under microscopic

a.—*Tension* (*100*×).

b.—*Zero load* (*100*×).

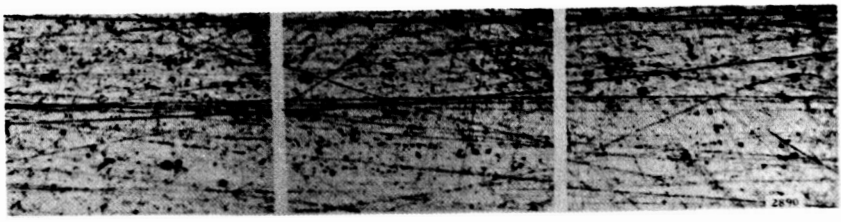

c.—*Compression* (*100*×).

FIGURE 11.—*Cavitation damage in brass vibratory specimens after 10-second exposure.*

examination, all specimens showed approximately uniform radial damage distribution over the damaged area. For comparison, figure 12 shows a heavily damaged specimen. Proficorder traces across its damaged area indicate that damage depth is again approximately uniform (ref. 2).

Comparing the short-duration specimens in detail, the pit-number density is greatest for the tension specimen (fig. 11*a*). There is a greater number of small pits than of large ones, as is typical in cavitation tests. The specimen with zero applied load (fig. 11*b*) has a somewhat larger number of small pits than the tension specimen, but the number and size of large pits are about the same. The compressive specimen (fig. 11*c*), however, shows a definite decrease in the number of both small and large pits.

Comparing the results from the vibratory facility with those from the mercury loop, the effects of externally applied stress are about the same even though specimen shape, material and fluid properties, and cavitation field differed drastically. In both tests the effect of the compression on damage in the early stages is to strongly decrease the number of small pits, with less effect on larger pits. Even in the early stages, however, the compressive force does not totally alleviate the damage. Rather, it appears to increase the threshold bubble energy required for creating a pit, thereby decreasing most strongly the number of small pits. The material is still vulnerable to higher energy bubble collapses, which cause the larger pits. It thus appears that the "incubation period" is increased by a compressive preload.

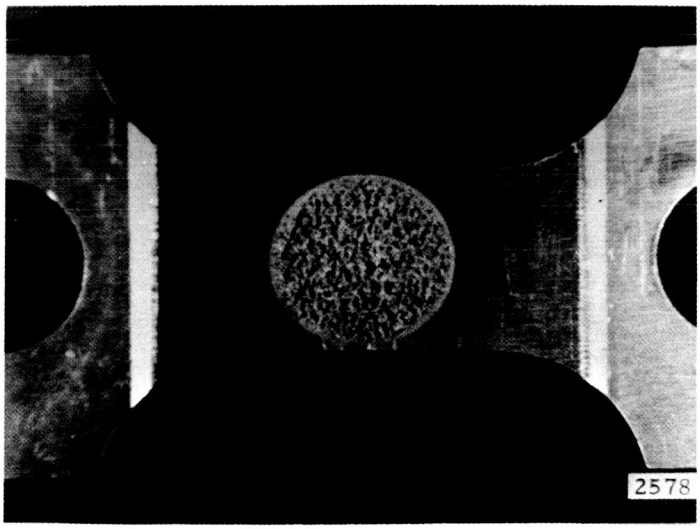

FIGURE 12.—*Center damage area of a specimen with a reduced cross section prior to tensile pull.*

Additional examples of early damage on metallic specimens were obtained using a plated specimen of 304 stainless steel. This experiment was suggested by the previous work of Noell (ref. 6) and Wood (ref. 7), who used a lacquer film coating to quickly indicate areas of maximum vulnerability to cavitation damage. Our water loop and associated test venturi were used in this investigation. Venturi throat velocity was 50 ft/sec with the cylindrical specimen (fig. 5) placed across the venturi. Several lacquer coatings were investigated. However, since these did not provide adequate bonding to the 304 stainless-steel specimen, electroplated cadmium films of various thicknesses were tried. These plated specimens were exposed to the cavitation field of the venturi for a 15-minute duration and then examined microscopically. As in the previously described mercury tests, the damage appeared on the sides and downstream portions of the cylinders. Pressure profiles and flow-regime photographs which enabled prediction of these damage areas were reported previously (refs. 2 and 6). Unlike the specimen from the mercury loop, only a small number of distinct circular holes or pits were found. Figure 13 shows the effect of varying thickness of the cadmium plate. A complete removal of cadmium at the pit center occurred for the thinner platings (fig. 13*a*, *b*). For thicker plating (fig. 13*c*), the damage does not extend completely through the plating.

In figure 13*b* a raised rim around the circular damaged area appears. Figure 13*c* shows areas where the cadmium has been partially dislodged. Close examination of these pits (fig. 13*c*) shows small circular areas (indicated by arrows and outlined in black ink for easier visualization) near the center of the damaged areas suggesting a very local circular area of most intense attack, as if the surface had been impacted by a microjet of liquid.

Figure 14 shows more detail of the pits in the thinner platings. The central area of each pit, void of all plating material, is surrounded by an outer area from which only a minor portion of the plating has been removed. Figure 14*a* is an enlarged photo of the most central pit in figure 13*a*. Its diameter is 0.6 μm. The complete symmetry of this central region from which the cadmium has been removed is shown. Such excellent symmetry strongly indicates that the material removal has been accomplished by a single (rather than multiple) impact.

These pictures strongly substantiate the theory that cavitation damage even in a flowing system may be created by liquid microjets generated during bubble collapse, rather than by spherical shock waves radiating from the bubble collapse center. The type of damage shown cannot easily be attributed to such shock waves, which would merely press the cadmium plate into the surface (as was demonstrated by impacting steel shot against a similar surface) rather than "washing it off." This damage is much more easily understood as the result of the radial velocity from a

high-velocity impacting liquid jet. Selected pictures of this type have been published previously by this laboratory (ref. 9) in support of this theory.

Metallurgical Examination of Damage Pits

A metallurgical examination of the region of the damaged surfaced area of the tension and compression specimens was made. SAE 660, a cast

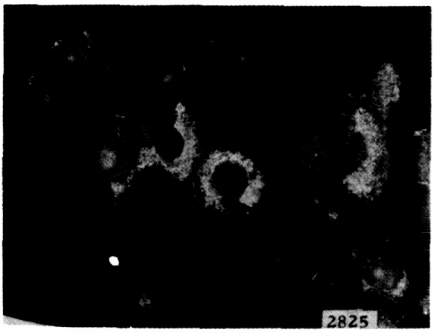

a.—*Coating thickness:* 2.5×10^{-5} *inches* (*120*×).

b.—*Coating thickness:* 5×10^{-5} *inches* (*note raised rim*) (*120*×).

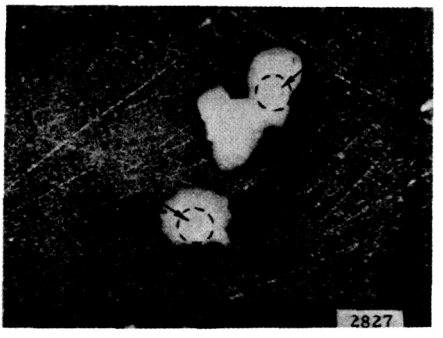

c.—*Coating thickness:* 5.5×10^{-4} *inches* (*small circles marked by arrows indicate a point of impact of a central jet*) (*120*×).

FIGURE 13.—*Effect of increasing cadmium coating thickness of stainless steel tubular pin specimens on water-loop cavitation pits.*

bearing bronze, and O.F.H.C. copper were tested for this purpose in the vibratory rig. Test duration was sufficient to provide relatively large MDP. Figure 15 illustrates the method of sectioning. The specimens were polished, etched, and then photographed at 400 diameters.

Figure 16 is four photomicrographs of a damaged SAE 660 specimen, showing both transverse and longitudinal sections. The interior "holes" are porosity in the cast material. This specimen had been tested under

a.—*Coating thickness: 2.5×10^{-5} inches (enlargement of central pit) (500×).*

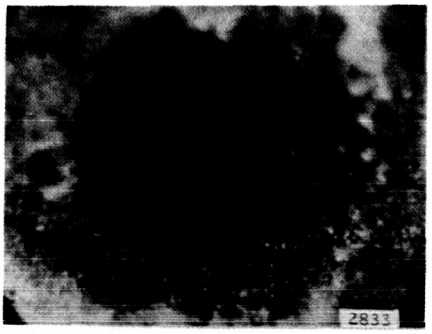

b.—*Coating thickness: 5×10^{-5} inches (120×).*

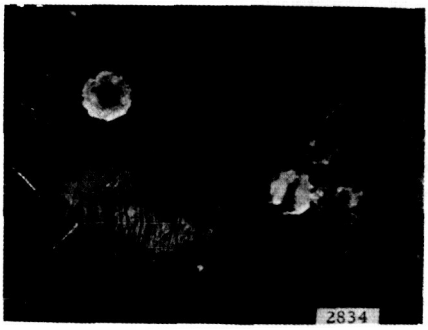

c.—*Coating thickness: 5×10^{-5} inches (note difference in area around pits) (120×).*

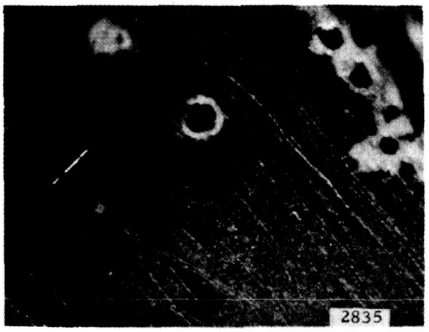

FIGURE 14.—*Cavitation pits in coated specimens showing material removal.*

FIGURE 15.—*Cutting directions on damaged specimens.*

a.—*Transverse (400×).*

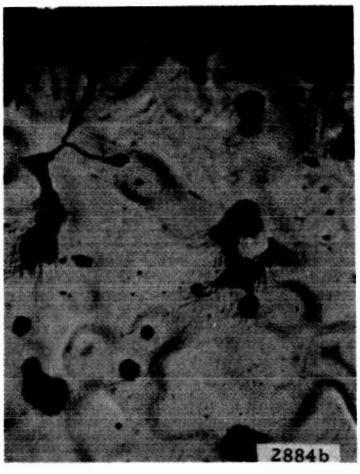

b.—*Transverse (400×).*

c.—*Longitudinal (400×).*

d.—*Longitudinal (400×).*

FIGURE 16.—*Photomicrographs of cavitation damage area of zero-load SAE 660 vibratory specimens.*

zero applied load. In the section in the transverse direction (fig. 16*a*, *b*) only a few cracks are visible. Slip lines, however, can be seen in photograph *a* at the base of the pit on the top right. Slip lines are also visible in photographs *b*, *c*, and *d*, indicating that the material adjacent to the pits has experienced considerable cold work. In photographs *a* and *b*, the slip lines appear almost perpendicular to the pit apex.

The longitudinal photographs (fig. 16*c*, *d*) show some evidence of microcracks at the base of the pits. In the center of photograph *d*, a large pit has at its apex a number of microcracks emanating in different directions. There are also slip lines on either side of the pitted region, particularly to the right of the apex, indicating that considerable cold work was done in this region. In figure 17, *a* and *b* are photomicrographs of SAE 660

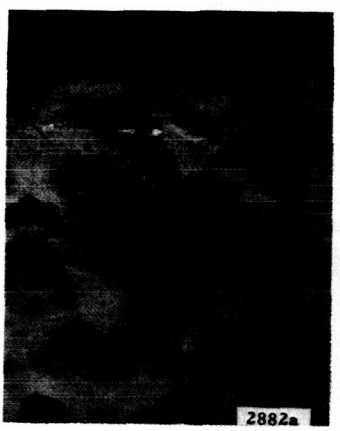

a.—*Compression—longitudinal* (400×).

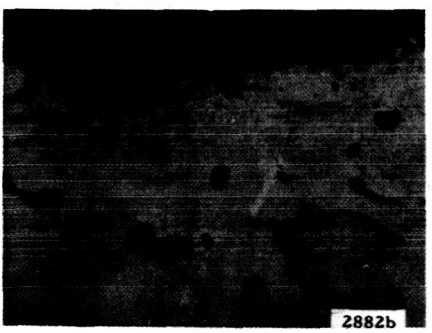

b.—*Compression—transverse* (400×).

c.—*Tension—transverse* (400×).

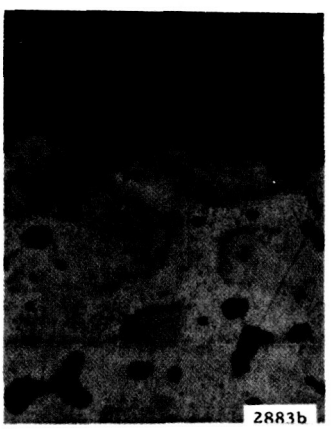

d.—*Tension—longitudinal* (400×).

FIGURE 17.—*Photomicrographs of cavitation damage area of tension and compression SAE 660 vibratory specimens.*

specimens tested under compressive load, while *c* and *d* are for a tensile specimen. In both stress modes the longitudinal pictures (*a*, *d*) show the microcracks from the area of the pit apex running vertically to the surface, and the transverse pictures (*b*, *c*) show the microcracks angled off from the pitted surface. None of these photos show slip lines, and there is no apparent difference between specimens tested under compressive or tensile load.

In figure 18, photos *a* and *b* show a copper specimen damaged with zero applied force, and photos *c* and *d* show a copper specimen damaged under

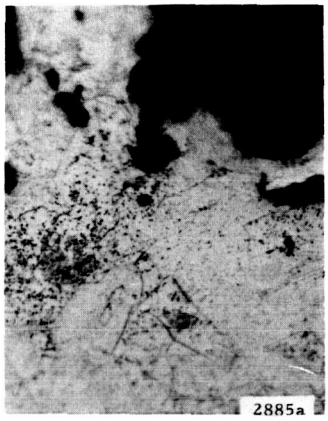

a.—*No force—transverse* (*400*×).

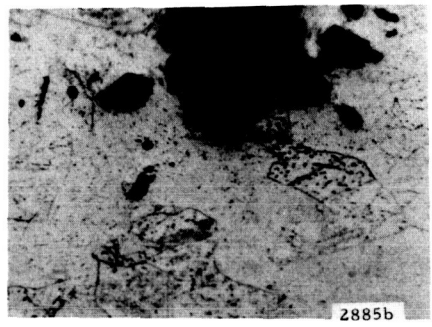

b.—*No force—longitudinal* (*400*×).

c.—*Tension—transverse* (*400*×).

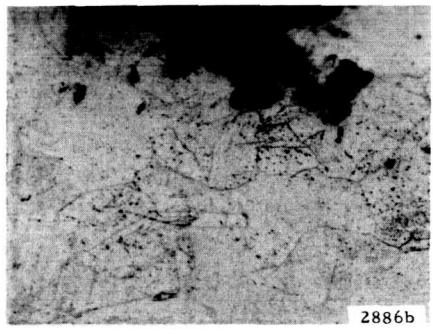

d.—*Tension—longitudinal* (*400*×).

FIGURE 18.—*Photomicrographs of cavitation damage area of tension O.F.H.C. copper vibratory specimens* (*400*×).

tensile load. In *a* and *b* there appears to be no difference between the transverse direction (*a*) and the longitudinal direction (*b*). There are, however, a few small microcracks at or near the apex of the damage pits. There are no discernable slip lines in these photographs, perhaps indicating little or no work hardening of the damaged surface.

Photos *c* and *d* of figure 18 also show no slip lines. However, both the transverse (*c*) and longitudinal (*d*) directions show larger, more prominent microcracks emanating from the base of the damage pits. As for the SAE 660, the cracks in the longitudinal direction appear to come away from the pits at an angle almost perpendicular to the centerline of the pit.

Figure 19 shows both the transverse (*a*) and longitudinal (*b*) directions of a copper specimen cavitated in compression. Close examination of the photographs reveals a number of microcracks at the base of the damage pits. These seem to start at the apex of the pit and continue until they intersect a grain boundary, at which point they terminate. The longitudinal picture again shows the direction of the cracks to be perpendicular to the surface.

Photomicrographs for brass specimens (not shown) give results similar to those for copper. There were, in all cases, microcracks in the region of the damage pits, but no slip lines. The damage is thus accompanied by two possible effects: (1) microcracks emanating from the base of the damage pits and (2) cold work or strain-hardening, depending on the material just below the damage surface. There appears to be no difference in the number of microcracks or their appearance in specimens tested.

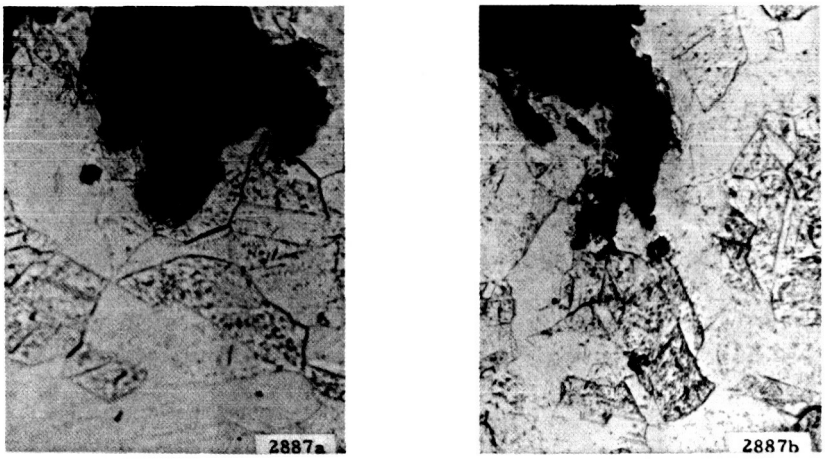

a.—*Transverse* (*400*×). b.—*Longitudinal* (*400*×).

FIGURE 19.—*Photomicrographs of cavitation damage area of compression O.F.H.C. copper vibratory specimens.*

under compression, tension, or zero load for these relatively heavily damaged specimens. This is consistent with the previously stated finding that after the surface has been broken the effect of the externally applied compressive stress is diminished.

CONCLUSIONS

In the early portion of a test when the materials were subjected to an external compressive stress, a substantial decrease in the number density of small pits was found. In tests run under compression, there was little difference between the mercury facility and the vibratory facility. The application of a tensile load in both the mercury facility and the vibratory facility produced very little or no difference in the amount of damage compared to that incurred under zero load.

Photographic investigation of individual pits shows that they are approximately circular. Such photographs strengthen the hypothesis that these pits are caused by the impact of liquid microjets generated during bubble collapse rather than by spherical shock waves radiating from the center of collapse.

Photomicrographs of different materials indicate two manifestations of damage immediately beneath the surface: (1) microcracks emanating from the apex of the pit and (2) areas of cold work just adjacent to the pit, depending on the material used.

The effect of an externally applied compressive stress appears to diminish after the damage has initially disrupted the surface. This is apparent because little or no difference in the microstructure below the pits was seen for the different stress modes after substantial damage was incurred.

REFERENCES

1. KEMPPAINEN, D. J., AND F. G. HAMMITT, Effects of External Load on Cavitation Damage. *Proc. IAHR Symposium* (Kyoto, Japan), September 1969; also available as ORA Technical Report 01357–5–T, Mech. Eng. Dept., Michigan U.
2. KEMPPAINEN, D. J., *Prestress Conditioning and its Effects on Material Attrition in a Cavitating Environment.* Professional Engineering Degree dissertation, Nucl. Eng. Dept., Michigan U., June 1969; also available as ORA Technical Report 01357–7–T, Michigan U.
3. GARCIA, R., *Comprehensive Cavitation Damage Data for Water and Various Liquid Metals Including Correlations with Material and Fluid Properties.* Ph.D. dissertation, Nucl. Eng. Dept., Michigan U., August 1966; also available as ORA Technical Report 05031–6–T, Michigan U.
4. ROBINSON, M. J., *On the Detailed Flow Structure and Corresponding Damage to Test Specimens in a Cavitating Venturi.* Ph.D. dissertation, Nucl. Eng. Dept., Michigan U., August 1965; also available as ORA Technical Report 03424–16–T, Michigan U.

5. HAMMITT, F. G., AND D. J. KEMPPAINEN, Cavitating Flow Past Transverse Cylinder in Venturi Diffuser with Water and Mercury. *Proc. 3rd Conference on Hydraulics and Hydraulic Machinery* (Budapest, Hungary), September 1969, pp. 255–264.
6. NOELL, G. L., *Cavitation Sensitive Coating Evaluation.* Pratt and Whitney Aircraft-CANAL, Technical Memorandum No. 878, June 1965.
7. WOOD, G. M., R. S. KULP, AND J. V. ALTIERI, JR., Cavitation Damage Investigations in Mixed Flow Liquid Metal Pumps. Pratt and Whitney Aircraft-CANAL, *Proc. Symposium on Cavitation in Fluid Machinery,* Winter Annual Meeting ASME (Chicago), November 1965.
8. HAMMITT, F. G., J. F. LAFFERTY, R. CHEESEWRIGHT, M. T. PITEK, D. J. KEMPPAINEN, AND T. M. MITCHELL, Laboratory Scale Devices for Rain Erosion Simulation. *Proc. 2nd Meersburg Conference on Rain Erosion,* March 1967; also available as ORA Technical Report 08153-3-T, Nucl. Eng. Dept., Michigan U.

DISCUSSION

F. GILMAN (Worthington Corporation): I discovered a paper which was not referenced by the authors; the mechanism involved may not be very closely related, but the subject is the effect of shot peening the surface of metals in an attempt to improve cavitation resistance. The paper is by Nicholas Grossman and appeared in ASTM Bulletin No. 183 of July 1952. The end of the abstract states, "In the present study the effect of shot peening on the rate of cavitation damage is investigated. Two types of steel and one of brass were tested. It was found that the damage which was measured by rate of weight loss per unit time was decreased by shot peening. The amount of decrease varied from 7 to 58 percent for the different materials."

J. DUSSOURD (Ingersoll Rand): I have always been a little skeptical of the damage theory which is the result of the physical impact of high-velocity jets, and I tend to be in favor of also viewing the importance of the electrochemical effect. I would like to raise some questions concerning some of the data. For example, the last slides show no effect of work-hardening on the surface, but you show deep penetration of the damage inside the structure. It seems that this would suggest that there are some effects which are not necessarily mechanical in nature. One is prone to think that maybe some other effects are really more important than we may believe. Also, it is disturbing that there are many bubbles but very few make individual pits.

D. REEMSNYDER (NASA Lewis Research Center): Although this paper contains some interesting data on cavitation damage, the results are somewhat confusing.

It would be helpful if the authors would comment in more detail on the discrepancy between the effects of compressive stress on long-term damage results observed in this investigation and those observed in previous work (ref. 1). For the long-term vibratory specimens of this investigation, the cavitation damage resistance of both copper and aluminum decreased due to the impressed radially symmetric compressive stress. However, the long-term cavitation damage resistance increased for the materials of reference 1, and the *initial* damage rate of the aluminum specimens *only* increased from that of the nonstressed specimen in this investigation. Why is there a discrepancy in the initial damage

rates of aluminum and copper? Perhaps there are factors other than material and direction of applied stress that affect the cavitation-damage resistance of a material.

The paper indicates that a stationary-specimen vibratory cavitation test facility was utilized in this investigation. A cavitation field is induced on the oscillating exponential horn tip, and the transmission and collapse of this field on the stationary test specimen may be dependent on gap (~.018 in.), frequency, material, fluid, gas content, pressure level, and/or the distribution of the cavitation field. It would be of interest to have the authors comment on the comparison of cavitation damage results obtained from a stationary-specimen and an oscillating-specimen vibratory test facility.

HAMMITT (author): The authors would very much like to thank the various discussors for their interesting comments. Some of these are actually in the form of supplying additional interesting input, and no reply is required. Others raise issues too complex to be handled briefly. However, we will attempt to summarize our view on some of the issues raised.

We agree that there are no doubt factors other than material and applied stress which affect cavitation damage, and also that such damage is not entirely the result of mechanical effects. However, for the observations discussed in the paper, we believe that mechanical effects predominate. In the field, mechanical effects can be more or less dominant depending on their intensity and the corrosivity of the environment. The latter can certainly be very important in some cases.

The photomicrographs from the present paper showing effects apparently well below the surface are misleading because of their large magnification. Actually, the effects in these tests are concentrated very close to the surface. It has been indicated that sometimes labyrinthine-type damage is found after long exposure in field tests. We agree that corrosive effects may well be very important in these cases.

We also agree with Mr. Dussourd that there are many bubbles and only a few pits. We interpret this as an indication of the very complex chain of events required to make a collapse damaging, involving the correct combination of bubble size, wall distance, velocity and pressure profiles in the flow, etc., necessary to generate a microjet with the correct orientation and intensity. Further light is thrown on this subject by work recently completed in our laboratory (refs. D–1 and D–2).

We believe that in some cases the effects of applied stress on cavitation damage rates can be quite important, while in others they are not. However, this is a factor which should at least be considered, and it may in some cases be possible to significantly inhibit the onset of major cavitation damage in this way.

In the present vibration damage tests, we used the stationary-specimen arrangement because it made feasible the application of applied stress. We have also used this method, as have others, to test materials which by their nature are not suitable for the usual vibratory arrangement. The damage rate does depend on amplitude, frequency, and gap distance, as well as other parameters. For the frequency (20 kHz) and amplitude of our facility (2 mils), we have found that the damage rate peaks at about 18 mils gap distance and, hence, is relatively insensitive to gap distance in this range. There is insufficient data available to allow a meaningful comparison between material rankings obtained in this test and in the conventional vibratory test. There is no reason to believe that the rankings should be widely different except for the fact that, in past experience, almost any change in test parameters for any type of cavitation test has appeared to provoke relatively large differences in relative material damage rates.

REFERENCES

D–1. KLING, C. L., *A High-Speed Photographic Study of Cavitation Bubble Collapse.* Ph.D. dissertation, Nucl. Eng. Dept., Michigan U., 1969.

D–2. KLING, C. L., AHD F. G. KAMMITT, A Photographic Study of Spark-Induced Cavitation Bubble Collapse. *Trans. ASME, J. Basic Eng.*, 1971–1972.